A SAM BEARING BALL INSPECTION SYSTEM

C-H. Chou, P. Parent, and B. T. Khuri-Yakub

Ginzton Laboratory, W. W. Hansen Laboratories of Physics
Stanford University, Stanford, CA 94305-4085

INTRODUCTION

Ceramic bearing balls have great potential for replacing steel bearing balls in most applications because of their lower weight, larger strength at high temperatures, and abundance of raw materials. However, ceramic materials are brittle, and the advantages of ceramic parts can be lost if small surface cracks and bulk defects are present in part. This work will report on a method we developed to detect small sub-micron surface cracks in ceramic bearing balls. We present a theory to calculate the scattering from these small "trenches" or cracks, and we will present an amplitude and phase measuring acoustic microscope capable of detecting these defects. We will present results of "line scans" across cracks in ceramics bearing balls where the balls are rolled under the stationary transducer.

THEORY

In order to predict the scanning acoustic microscope's ability for detecting and imaging narrow surface depressions, we calculate the scattering from trenches using a theory similar to the one dealing with the imaging of trenches with a confocal scanning optical microscope [1,2].

As shown in Fig. 1, when an acoustic beam illuminates the surface trench (depression) with width L and depth h , the reflected beam can be considered as the sum of a homogeneous wave (i.e., the wave reflected from a perfect plane boundary) and a scattered wave (caused by the depression). That is:

$$V_r = V_{hom} + V_s \tag{1}$$

where V_r , V_{hom} , and V_s are the particle velocities in the z-direction of reflected, homogeneous and scattered waves, respectively.

The boundary conditions at $z = 0$ are:

$$V_{tr} = V_{inc} + V_r = V_{inc} + V_{hom} + V_s \tag{2}$$

$$\partial V_{tr} / \partial z = \partial V_{inc} / \partial z + \partial V_r / \partial z = \partial V_{inc} / \partial z + \partial V_{hom} / \partial z + \partial V_s / \partial z \tag{3}$$

where V_{inc} is the particle velocity in the z-direction of the incident wave and V_{tr} is that of the wave inside of the trench.

Review of Progress in Quantitative Nondestructive Evaluation, Vol. 9
Edited by D.O. Thompson and D.E. Chimenti
Plenum Press, New York, 1990

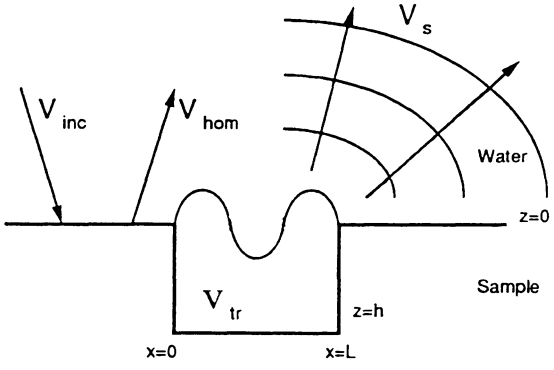

Fig. 1. Trench structure for scattering simulation.

For the samples with much higher acoustic impedance (such as Si_3N_4) than the working couplant (water), at the boundary, we have:

$$V_{hom} = - V_{inc} \tag{4}$$

$$\partial V_{hom} / \partial z = \partial V_{inc} / \partial z \tag{5}$$

Therefore, Eqs. (2) and (3) can be simplified as:

$$V_{tr} = V_s \tag{6}$$

$$\partial V_{tr} / \partial z = 2\partial V_{inc} / \partial z + \partial V_s / \partial z \tag{7}$$

In order to solve V_s, we decompose V_s at $z = 0$ into spatial frequency components, and then decompose each component into trench modes:

$$V_s = \sum_{n=1}^{N} \int \int A_n(p,q) \sin(n\pi x/L) e^{-jkpx} e^{-jkqy} dpdq \tag{8}$$

where k is the wave number. To satisfy Eq. (6), we can write:

$$V_{tr} = \sum_{n=1}^{N} \iint A_n(p,q) \sin(n\pi x / L) \left[\sin(\gamma_n (z+h) / (\sin \gamma_n h)\right] e^{-jkpx} e^{-jkqy} dpdq \tag{9}$$

where:

$$\gamma_n = k\sqrt{1 - p^2 - q^2} \tag{10}$$

$\partial V_{inc}/\partial z$ can also be decomposed as:

$$\partial V_{inc} / \partial z = \sum_{n=1}^{N} \iint D_n(p,q) \sin(n\pi x / L) e^{-jkpx} e^{-jkqy} dpdq \tag{11}$$

As in Ref. 2, $A_n(p,q)$ can be solved from the following equation:

$$\sum_{n=1}^{N} H_{mn}(q) A_n(p,q) = D_m(p,q) \tag{12}$$

where $H_{mn}(q) = (1/2)\gamma_n \cot(\gamma_n h)\delta_{mn} - \Gamma_{mn}(q)$.

$$\Gamma_{mn}(q) = \frac{jk^2}{\pi L}\int_{-\infty}^{\infty} \frac{(m\pi/L)(n\pi/L)\sqrt{1-p^2-q^2}}{\left[k^2p^2-(m\pi/L)^2\right]\left[k^2p^2-(n\pi/L)^2\right]}\left[e^{-j(kpL-m\pi)}-1\right]\left[e^{-j(kpL+n\pi)}-1\right]dp \tag{13}$$

The received signal by the transducer of the SAM is:

$$\begin{aligned} v &= v_s + v_h \\ &= 2\int_{s_1} V_s^* \frac{\partial V_{inc}}{\partial z} ds + 2\int_{s_1} V_h^* \frac{\partial V_{inc}}{\partial z} ds \end{aligned} \tag{14}$$

where * denotes a complex conjugate and s_1 is the sample plane $z = 0$. Since the incident wave at $z = 0$ depends on the focal location (x_0,z_0) of the acoustic beam, v is a function of x_0 and z_0 .

Figure 2 shows the theoretical line scan results across a trench with 1 μm in width and 1 μm in depth operating at 118 MHz with a 0.8 F-number lens focused on the top surface. From the theoretical prediction, the phase variation is 0.8° and the amplitude variation is less than 0.1% for this case.

REAL TIME DIFFERENTIAL PHASE MEASUREMENT SYSTEM

We reported on our amplitude-phase measurement system operating in the range of 1-200 MHz at the IEEE Ultrasonics Symposium last year [3]. In order to inspect the whole surface of a bearing ball, we developed a rotation apparatus capable of rotating spherical objects such that its whole surface is inspected by a stationary microscope lens. Unfortunately, vibrations in the scanning stage raise the noise level to ±4° for phase and 2% for amplitude measurements at an operation frequency of 118 MHz , respectively. These noise figures are much higher than the phase and the amplitude variation due to a 1 μm x 1 μm surface depression which was theoretically predicted to be 0.8° in phase and 0.1% in amplitude at this frequency. In order to detect surface defects of a size around 1 μm x 1 μm we must reduce the phase measurement noise level below ±0.5°.

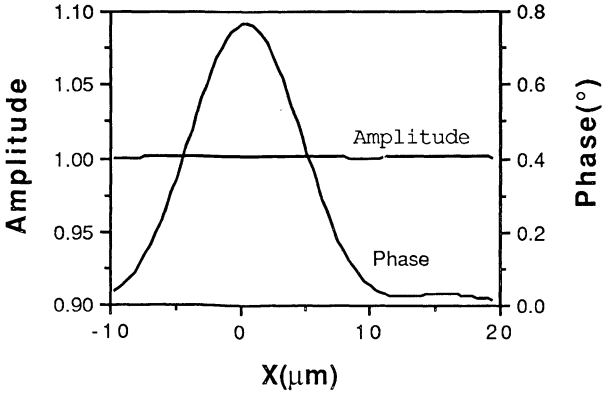

Fig. 2. Theoretical results of line scan of a 1 μm wide, 1 μm deep trench. Operating frequency = 118 MHz, F# of lens = 0.8 , focused on top.

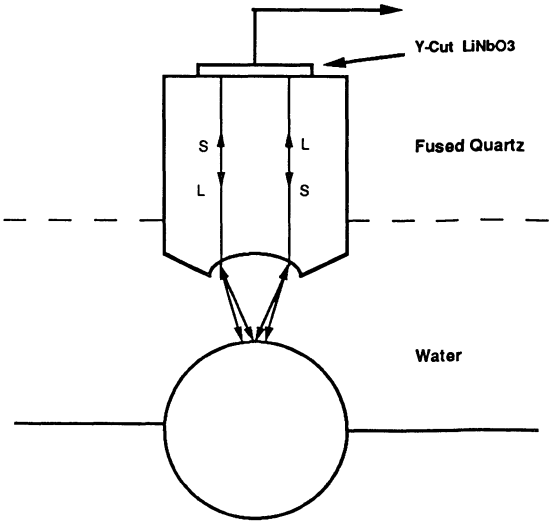

Fig. 3. Schematic of mixed mode transducer for differential phase measurement.

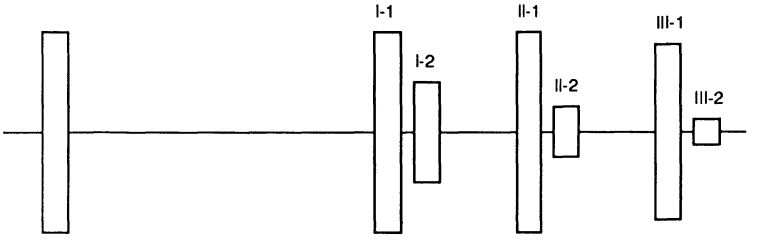

Fig. 4. Schematic of the received signals by the mixed mode transducer. I-1 -- LL wave from the lens-water interface. I-2 -- LL wave from the sample. II-1 -- LS wave from the lens-water interface. II-2 -- LS wave from the sample. III-1 -- SS wave from the lens-water interface. III-2 -- SS wave from the sample.

To reduce the noise level, we developed a differential phase measurement system. As shown in Fig. 3, a mixed mode transducer was used to generate both longitudinal and shear waves in the buffer rod simultaneously. Because of mode conversion when reflected from the lens-water interface, the signals traveling inside the buffer rod are separated into three groups, i.e., LL (both ways longitudinal), LS (one way longitudinal, the other shear), and SS waves (both ways shear), as shown in Fig. 4. Each group has one signal reflected from the lens-water interface, followed by a weaker signal which is transmitted into water and reflected from the surface of the sample. The wave groups LL, LS and SS signals are focused at different locations in the water. When we focus one group, for instance LL, on the sample surface to measure a defect, either one of the other two groups is defocused and can be used as a reference for the signal of interest. In our experiment, we focused the LL wave on the surface of the sample and used the LS wave as a reference. Because both beams propagate the same path in the water, their phase difference eliminates the effects of the scanning vibration and the temperature fluctuation in water. As shown in Fig. 5, we separate the LL signal and LS reference into two channels, and process the signals in the same fashion as for a single channel system. The computer is used to compare the signals from the two channels and to calculate the amplitude and phase of the difference signal. The resultant differential amplitude and phase are also converted into an analog signal, and can be monitored by an oscilloscope or recorded on a x-y recorder in real time when the sample is scanning.

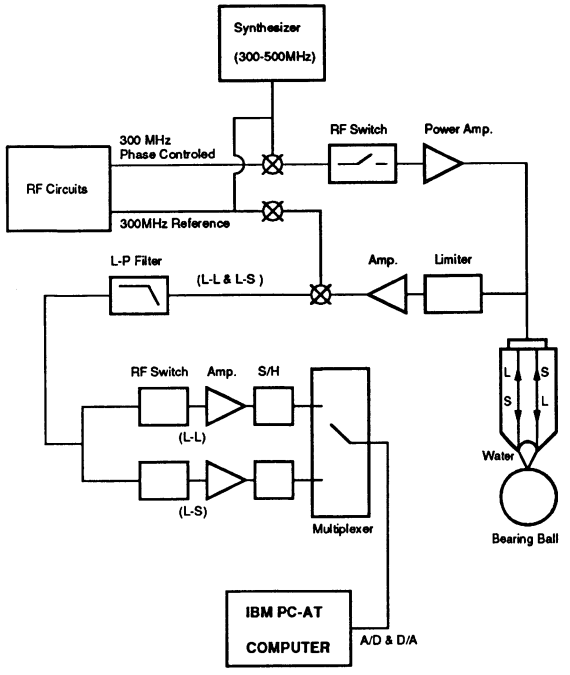

Fig. 5. Block diagram of differential phase measurement system.

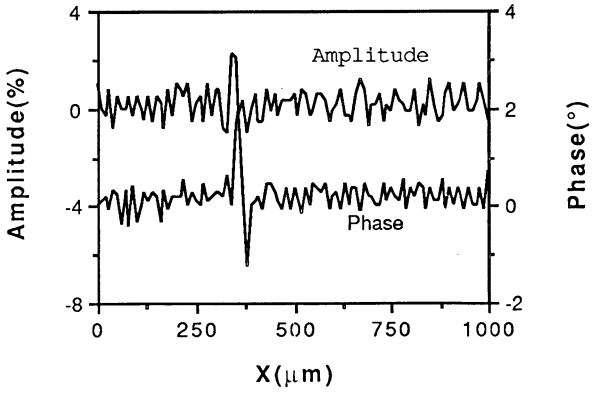

Fig. 6. Experimental results of a line scan across a small surface depression on a Si_3N_4 bearing ball.

EXPERIMENTAL RESULTS

We used a rotating system to provide the inspection of the bearing balls. This system is driven by two stepper motors; the first rotates a rubber roller which rotates the ball, while the other translates the roller, giving a rotation of the ball in the orthogonal direction. With the differential phase measurement system, the total phase noise measured was reduced down to $\pm 0.4^{\circ}$, which allows us to be able to measure surface depressions of sizes above 1 μm x 1 μm. Figure 6 shows one example of such a measurement. The phase variation of the defect is 2.5°, which corresponds to a 2 μm (w) x 1 μm (d) depression, as predicted by theory. The amplitude variation is higher than the theoretical calculation, which is caused by the roughness of the defect edges.

CONCLUSION

We have demonstrates a differential phase measurement system which is insensitive to mechanical vibrations and temperature fluctuations. With this system, the phase noise is reduced to $\pm 0.4^{\circ}$, which allows us to detect defects of a size above 1 μm x 1 μm .

Also, a real-time data acquisition and display system is used to inspect bearing balls automatically . Some improvements of the scanning system are necessary for robust operation of the inspection system.

ACKNOWLEDGMENT

This work was supported by the Department of Energy on Contract No. DE-FG03-84ER45157.

REFERENCES

1. P. C. D. Hobbs, "Heterodyne Interferometry with a Scanning Optical Microscope," Chapter 6, Ph.D. Dissertation, Stanford University, Stanford, CA (August,1987).
2. G. S. Kino et al, "Confocal Microscopy of Trenches," to be submitted to Applied Optics.
3. P. Parent, C-H. Chou, and B. T. Khuri-Yakub, "Ball Bearing Inspection with an Acoustic Microscope," Proc. IEEE Ultrasonics Symposium (1988).